

NEUTRAL ION SOURCES IN PRECISION MANUFACTURING

Steven C. Fawcett

Optical Systems Branch, EB53, National Aeronautics and Space Administration
Marshall Space Flight Center, AL 35812

Thomas W. Drueding

Aerospace and Mechanical Engineering, Boston University
Boston, MA 02215

ABSTRACT

Ion figuring of optical components is a relatively new technology that can alleviate some of the problems associated with traditional contact polishing. Because the technique is non contacting, edge distortions and rib structure print through do not occur. This initial investigation was aimed at determining the effect of ion figuring on surface roughness of previously polished or ductile ground ceramic optical samples. This is the first step in research directed toward the combination of a pre-finishing process (ductile grinding or polishing) with ion figuring to produce finished ceramic mirrors. The second phase of the project is focusing on the development of mathematical algorithms that will deconvolve the ion beam profile from the surface figure errors so that these errors can be successfully removed from the optical components. In the initial phase of the project, multiple, chemical vapor deposited silicon carbide (CVD SiC) samples were polished or ductile ground to specular or near-specular roughness. These samples were then characterized to determine topographic surface information. The surface evaluation consisted of stylus profilometry, interferometry, and optical and scanning electron microscopy. The surfaces were ion machined to depths from 0-5 μm . The finished surfaces were characterized to evaluate the effects of the ion machining process with respect to the previous processing methods and the pre-existing subsurface damage. The development of the control algorithms for figuring optical components has been completed. These algorithms have been validated with simulations and future experiments have been planned to verify the methods. This paper will present the results of the initial surface finish experiments and the control algorithms simulations.

INTRODUCTION

In the new precision fabrication facility currently being implemented at Marshall Space Flight Center (MSFC), the ion figuring technology is being evaluated to complement traditional high precision material removal techniques. The use of neutral ion beams to remove selected material has been developed and is currently in use at a few commercial installations and research facilities [1-10]. These implementations typically use the process for final figure correction on meter class optical components. The new facility at MSFC will develop and evaluate this technique for producing the optics required on many of NASA's missions. The initial work focuses on the production of centimeter scale optics to achieve the extremely tight tolerances in a reasonable time. After the development work has been completed, the fabrication procedures will be optimized for the particular requirements of various missions. This technology is extremely important to advance the fabrication techniques used in the production of high precision components. The process has a wide variety of commercial applications in the areas of optics manufacturing as well as other potential uses in fields where components are required with precision figure and surface finish tolerances. The use of neutral ion sources for material fabrication is probably one of the key technologies for manufacturing in the next century.

Loose abrasive polishing and ductile regime grinding are two fabrication processes that can provide optical quality surface finish on a glass or ceramic mirror. Polishing usually involves loose abrasive particles working between a flexible pad and the mirror material, creating the desired surface characteristics by either frictional abrasion or chemical reactions or both. A newer fabrication procedure that can potentially be used for optical surface fabrication is ductile regime grinding [11-14]. In this technique, the substrate is formed on a precisely controlled fixed abrasive grinding machine. The process parameters are controlled to allow for material removal by plastic deformation instead of brittle fracture. Both polishing and ductile grinding can produce the angstrom level surfaces required by precision optical components. It should be noted that the ion figuring technique require that the mirror segments have optical quality surface finishes prior to figuring since the ion machining can not currently be utilized to improve the finish of components. Polishing and ductile-regime grinding will be evaluated as preliminary fabrication technologies, in which the contour accuracy of the component is achieved to within 1-2 μm of the final specification, and the component is finished to the final surface roughness specification. Subsequent ion-figuring will then be used to improve the contour accuracy while maintaining angstrom-level roughness.

The use of neutral ion beams to remove selected material has been developed for final figure correction on meter class optical components [5-8]. The technique has been developed for this size application with commercially available, three to five centimeter ion sources. These sources are utilized for the correction of large and middle spatial frequency errors on optical components. The procedure uses an interferometric contour subtracted from an ideal contour to produce a map of the figure errors. The process itself is based on a momentum transfer from previously ionized molecules of inert gas. This results in molecular level sputtering of the substrate material. The basic operation is depicted in Figure 1.

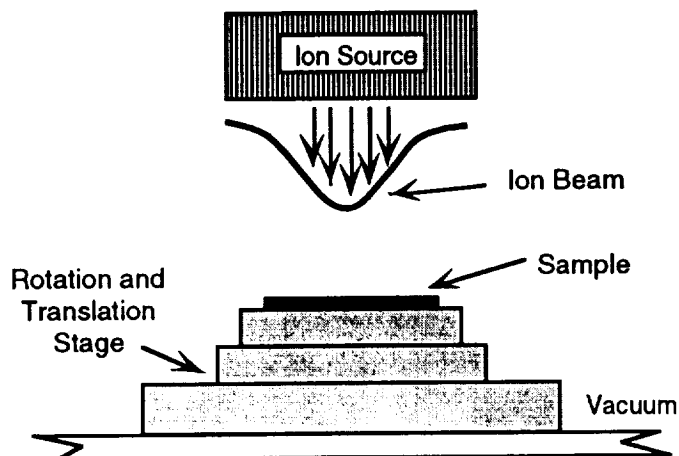


Figure 1 Schematic of ion figuring process. A semi-Gaussian ion function imparts the final figure contour on the substrate by computer controlled translation and rotation.

The new research facility at MSFC will focus on using the technique for the figuring of centimeter scale optics [15]. This facility was constructed around a surplus sputtering chamber obtained for this program. This chamber was retrofitted with a 3 cm, Kaufman filament type ion source [16]. This source is driven by a programmable power supply which can provide current densities to 10 mA/cm^2 . The basic system is shown in the computer model of Figure 2.

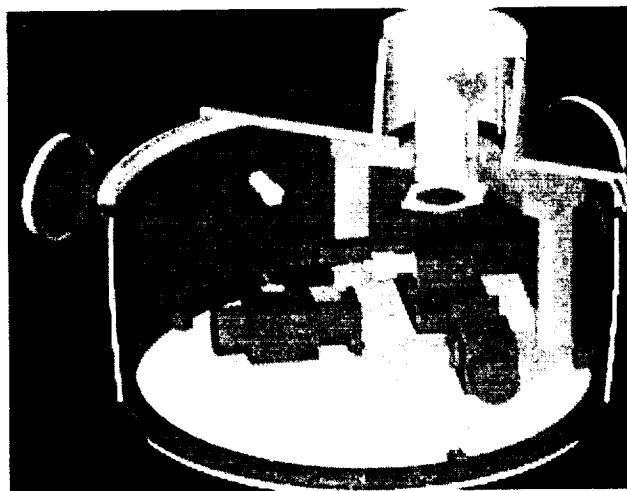


Figure 2 Solid model of the ion figuring system components.

The initial experiments were designed to evaluate the machining characteristics of Chemical Vapor Deposited silicon carbide (CVD SiC). The polished samples were 3 cm diameter and the ductile ground samples were 6 mm wide by 25 mm long rectangular pieces. The polished samples were processed by lapping with an oil based diamond compound. The ductile ground samples were obtained from the same batch as the polished samples. They were mounted on steel sample holders and ground in the ductile regime with a fixed abrasive diamond grinding wheel.

An experiment was performed to determine the beam current profile and hence the expected material removal rate on the CVD SiC samples. In this experiment, a polished, circular sample was located beneath the ion beam so that the edge of the sample would correspond with the point of maximum beam intensity. One half of the sample was masked to provide a reference surface for step height measurements. This process is depicted in Figure 3. Throughout these experiments, the ions were produced from Argon gas. After the sample was ion machined for a specified period, the relative height differences between the surfaces was measured with a Talysurf stylus profilometer and normalized with respect to time. Figure 4 shows a plot of the measured machining rate versus the distance from the beam center.

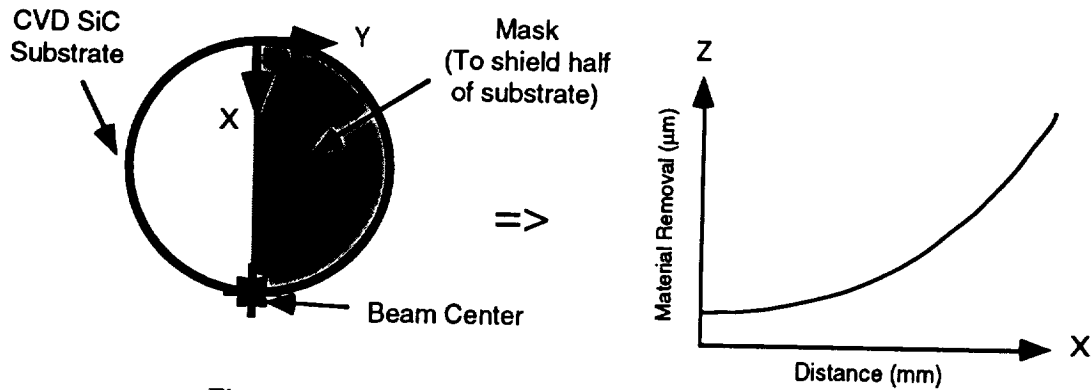


Figure 3 Masking technique for determining machining rate.

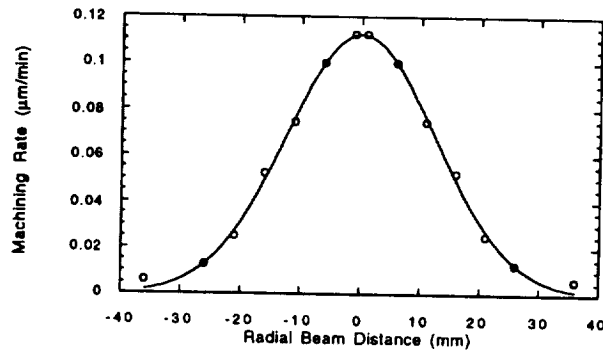


Figure 4 Machining profile of 3 cm ion source.

Once the samples were polished or ground, surface characterization measurements were made. Unmagnified, visual examination revealed no scratches or pits in any of the samples. Optical microscopy to 400 X only revealed an occasional fracture location and grooves on the ground samples caused by the grinding crossfeed, especially on sample D1. The samples were viewed with a scanning electron microscope (SEM). There were small ($\approx 100 - 200$ nm diameter) discontinuities visible in the SEM micrographs of the ground samples. On all the polished samples, small (~ 100 nm wide) scratches became visible. All the samples were measured to determine the surface roughness parameters prior to ion machining. It was determined that the surfaces roughness of the samples was below the noise floor of the Talysurf profilometer. The initial measurements were instead made on a WYKO optical profilometer to determine the surface roughness. Ductile ground sample "D4" was also measured by Mark Gerchman of Rank Taylor Hobson, Inc. on a Talystep stylus profilometer for verification. Multiple measurements were made for each sample and the results averaged. The RMS values from the WYKO data for an area approximately $235 \times 235 \mu\text{m}$ square ranged from $7.56 \pm 2.07 \text{ \AA}$ to $12.77 \pm 4.65 \text{ \AA}$ for the polished samples and from $12.87 \pm 4.94 \text{ \AA}$ to $52.25 \pm 34.51 \text{ \AA}$ for the ductile ground samples. The Talystep data for sample "D4" gave an average roughness of $13.14 \pm 5.24 \text{ \AA}$ RMS for a $150 \mu\text{m}$ linear trace.

SURFACE FINISH RESULTS

After the initial surface finish evaluation, the samples were ion machined in a fixed position with respect to the beam, so that the total depth profile at various positions on the sample surface could be correlated with the ion

machining depth profile plotted in Figure 4. These samples were then examined to determine the effect of the ion sputtering process. During machining, the samples could be viewed through a transparent port in the vacuum chamber. This examination revealed an interesting phenomenon: previously hidden damage on the polished samples became highly visible after only a few minutes under the beam. After machining, some of the samples showed extensive damage when examined under an optical microscope. The extent of this damage increased with an increase in ion machining depth. Optical micrographs revealed hemispherical pits uncovered by the ion machining process on the polished samples. The pits are believed to have been formed at the sites of sub-surface damage caused by the loose abrasive polishing with the larger grit diamond. The size of the pits are approximately 10 to 20 μm diameter which corresponds to the fracture size expected from the initial polishing stage with 15 μm diamond. Because of the lack of a controlled polish, it is probable that the fractures from previous grit sizes was not completely removed in subsequent steps and were left as sub-surface damage. These damage sites were then uncovered by the ion figuring. The micrographs of Figure 5 appears to verify the hypothesis that the pits are formed in the areas of sub surface fracture. Figure 5 shows a line of these hemispherical pits formed on an uncovered sub-surface scratch. These pits apparently follow a scratch line where fractures occur under the stresses induced while polishing with the larger grit sizes.

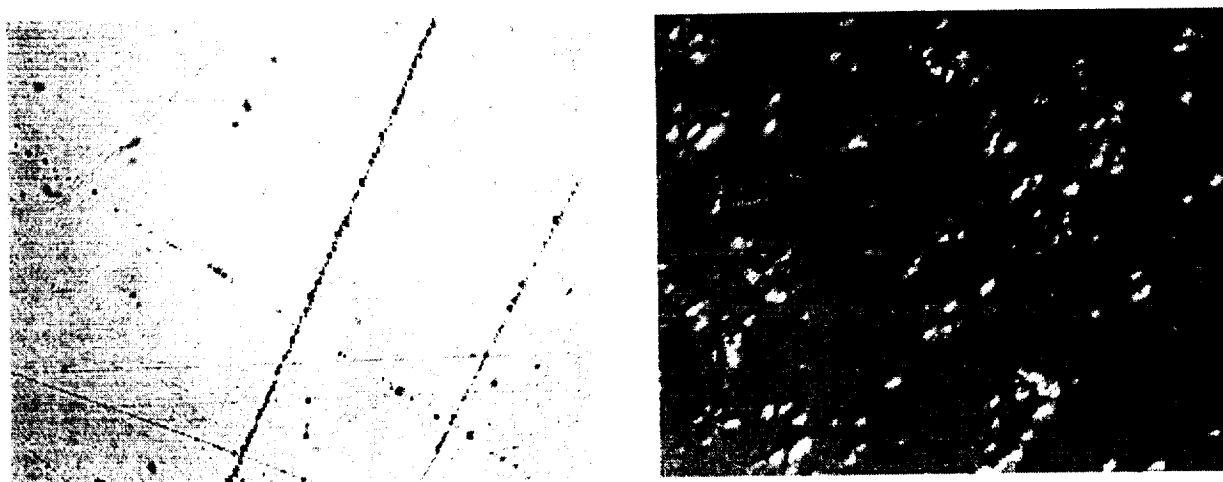


Figure 5 Optical micrographs of subsurface fracture revealed by ion machining on a polished CVD SiC sample (200 X left and 400 X right).

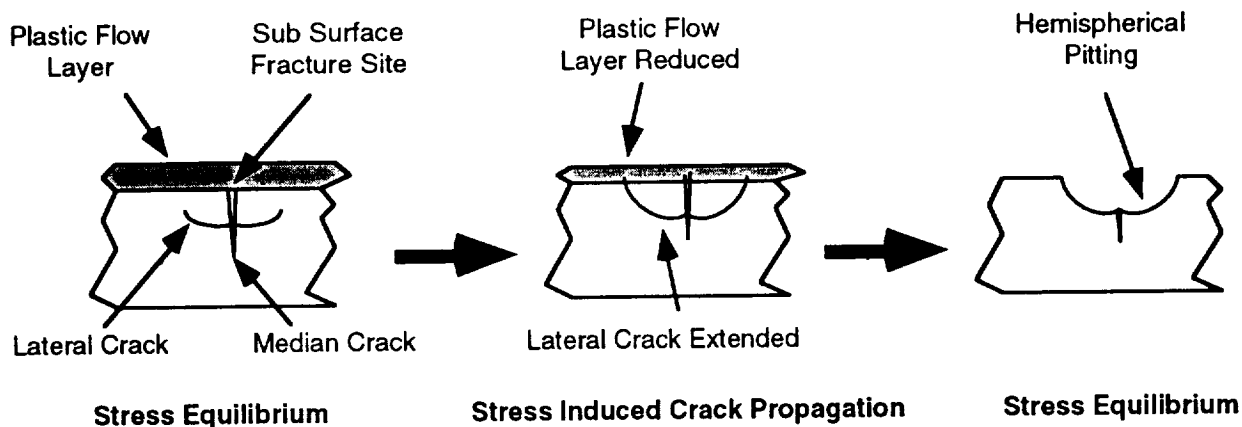


Figure 6 Schematic of the proposed crack propagation process. The layer that provided stress equilibrium is removed and the sub-surface crack propagates eventually reaching the surface.

It is believed that the pitting sites are formed when the lateral cracks caused by the forces of the individual diamond grits are uncovered. The lateral cracks may potentially propagate due to the removal of the plastic flow layer which initially provided the stresses required to maintain equilibrium. Figure 6 demonstrates this idea schematically. When the plastic layer is removed by the ion sputtering process, the equilibrium condition is modified by removal of the

compressive surface layer with the resulting increase in tensile stress below the surface, and the cracks grow. When the surface layer meets the extended lateral crack, the material above the crack is expelled, (releasing the residual stress) to reveal the hemispherical pits. The thermal loading inherent with the ion figuring process may be a contributing factor. The areal density of these fracture sites appears to directly correlate with the density of the ion beam current and hence with the machining depth.

The ground samples were also evaluated optically. The samples ground in the ductile regime showed only a few fracture sites in localized areas of the samples. These areas appeared to correspond with sites which may have undergone some scratching during the grind. However, most of the areas were free of fracture. The pits shown range from 3 to 8 μm diameter which is similar to the diamond grit size of 4 to 8 μm . The brittle ground sample "D1" showed some hemispherical pitting similar to the polished samples. Surface roughness measurements were also made on the figured samples. Prior to machining, six measurements were made at random locations for each of the samples with the WYKO optical profilometer. These results were averaged and are shown in Table 1.

Sample	WYKO Data (\AA)
P 1	7.56+2.07
P 2	7.95+0.62
P 3	10.5+5.31
P 4	12.77+4.65
D1	52.25+34.51
D2	15.78+4.02
D3	12.87+4.94
D4	17.45+2.07

Table 1 RMS surface finish of CVD SiC samples (WYKO measurement area approximately 235 x 235 μm).

After ion machining, the samples were again measured with the optical profilometer. Those samples exhibiting significant pitting (including all of the polished samples and two of the four ground samples) could not be measured with the WYKO optical profilometer. The steep slope of the pit edges exceeded the measurement capacity of the optical profilometer. Data was obtained from the WYKO for three of the ground samples that had relatively few pits (ductile ground samples D2, D3 and D4). The RMS surface finish measurements made over the entire surface were averaged to obtain $15.77 \pm 2.14 \text{ \AA}$ for sample D2, $17.98 \pm 4.06 \text{ \AA}$ for sample D3 and $23.01 \pm 6.95 \text{ \AA}$ for sample D4. The area of measurement for the samples was approximately 470 x 470 μm for D2 and 235 x 235 μm for D3 and D4. This surface roughness revealed no significant increases as a function of machining depth. Those samples that could not be measured with the optical profilometer were instead measured using a Talysurf stylus profilometer. This data at each ion machined depth was collected in four linear, 1 mm traces of the samples with no filtering. The RMS roughness average of each set of four traces is plotted against ion machining depth in Figures 7 and 8. Figure 7 shows the surface roughness as a function of ion machining depth for the polished samples. There is an obvious increase in the surface roughness at the greater machining depths. This roughness increase is primarily due to the pitting that occurred in these polished samples.

Sample "P4" does not show the same increase in roughness as the other polished samples. This sample was polished for a longer time than the others, suggesting that the observed pitting may be the result of rough-machining steps prior to polishing, and that the polished samples were not polished long enough to remove all prior damage. Figure 8 shows the surface roughness measurements for the ground sample D1. The other ground samples exhibited roughness that was below the noise floor of the Talysurf profilometer. The sample, D1, which was ground in the brittle regime, exhibits the same trend of increasing roughness with ion machining depth that was observed in the insufficiently polished samples. Before ion machining, D1 had a roughness of 52 \AA RMS. Also this sample had an abundance of damage sites that became visible under the optical microscope after ion machining. It should be noted that the vertical resolution of the Talysurf is 10 nm and results in the absence of measurements below this threshold in Figures 7 and 8. The pitting exhibited on the polished samples and the ground sample D1 prevented Wyko optical profilometry measurements for these samples.

DISCUSSION OF SURFACE FINISH EXPERIMENTS

From these results, it seems apparent that ion machining acts to expose, and possibly amplify, any pre-existing subsurface damage in specularly finished CVD SiC. This exposure of damage causes significant roughening of the surface, diminishing its optical quality. Both pre-finishing techniques, grinding and polishing, can be used to

generate specular surfaces. However, the *roughness* of the finished surface is not indicative of the extent of subsurface damage. All of the polished samples, and three of the four ground samples exhibited RMS roughness before ion machining that were below 20 Å. After ion machining to a depth of 5 μm, those samples having significant and visually apparent subsurface damage exhibited increases in RMS roughness to as much as 1400 Å, while those samples that showed no evidence of subsurface damage exhibited almost no increase in RMS roughness.

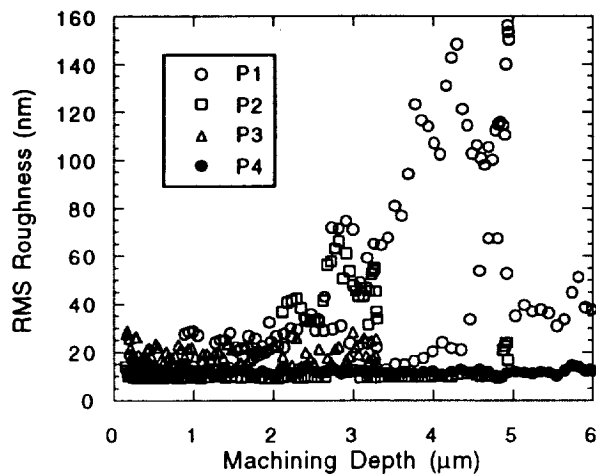


Figure 7 Surface roughness variation with ion machining depth for polished samples.

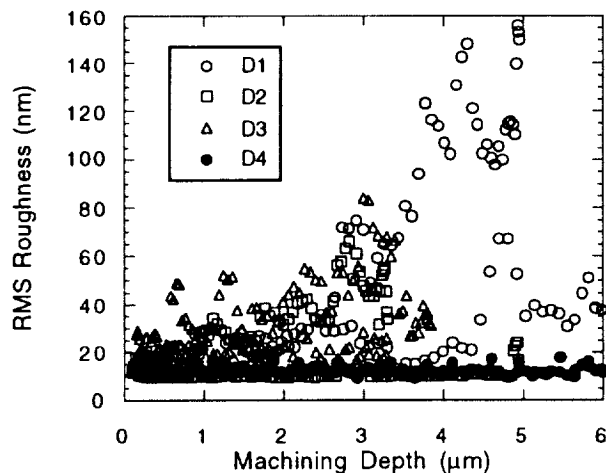


Figure 8 Surface roughness variation with ion machining depth for brittle ground sample D1.

The subsurface damage uncovered by ion machining might have been the result of rough machining processes prior to polishing or grinding, or they might have been introduced by these finishing processes themselves. The evolution of roughness in the polished samples, however, provides evidence suggesting that prior machining processes are responsible: the polished sample exhibiting the least amount of subsurface damage had been polished for at least twice as long as the other samples but no verifiable material removal measurements were ever made during the polishing. If the polishing process itself were a primary contributor to the subsurface damage, this sample would have been expected to exhibit at least as much damage as the others. It is perhaps not surprising that the subsurface damage from previous rough machining was not completely removed in the polished samples: the large value of hardness exhibited by SiC causes it to have an exceptionally low polishing rate. These polishing

experiments were conducted with diamond abrasive on a Kemet lap and with B₄C abrasive on a cast iron lap. Although it is possible to increase the polishing rate by polishing at a higher pad pressure, it is also possible that the increased polishing grain loading would itself result in polish-induced subsurface damage.

Ductile-regime grinding appears to be a good way to obtain the two prerequisites for ion machining: a specular finish and the absence of subsurface damage. It has been demonstrated in these experiments that it is possible to grind SiC to RMS roughness in the 10-20 Å range, without introducing any subsurface damage. If the grinding process is not carried out in the ductile regime, however, then the RMS roughness of the sample will increase with subsequent ion machining. An interesting result of these experiments is the observation that ion machining acts to expose subsurface damage in SiC. By itself, this process may be useful as a locally-destructive diagnostic technique for evaluating the subsurface damage in a specular component, in the same way that HF acid etching is used to evaluate subsurface damage in glass. Since acid does not readily etch SiC, ion machining can serve as a clean, efficient alternative for post-processing measurement of subsurface damage in ceramic components. These experiments provide strong evidence that ceramic mirrors could be produced by pre-finishing in a ductile machining process (either ductile-regime grinding or polishing), followed by ion machining. A distinct advantage of such a fabrication technique is that, at the end of the ion milling process, the mirror surface is atomically clean, and it is in a vacuum chamber. This means that the surface is ready for any subsequent coating processes that are to be performed on the mirror, processes that generally require atomic cleanliness and a vacuum environment anyway.

FIGURE CONTROL ALGORITHMS

An important step in the fabrication of an optical component involves the expensive and time consuming process of imparting a precise contour on the optic. Ion beam figuring provides a highly deterministic method for the final precision figuring of optical components with advantages over conventional methods. The repeatability of the process allows the possibility of single step figuring, resulting in significant time and cost savings. Unlike grinding, polishing and lapping, ion figuring is non-contacting and so avoids several problems including: edge effects, tool wear, and loading of the work piece. The work discussed here is directed toward the development of control algorithms for ion machining of small (≤ 10 cm diameter) optical components. The development of the algorithms has proceeded in three steps: 1) the development of control algorithms; 2) the use of a simulation to verify the methods and to identify important issues that are critical for the proper operation of the system 3) the integration of the controlling algorithms with the other components. Experimental testing of the system will then follow and includes the figuring of chemically vapor deposited silicon carbide (CVD SiC) and fused silica samples. An emphasis will be placed on CVD SiC that have been previously fabricated by ductile-regime grinding.

The ion figuring process involves bombarding a surface with a temporally and spatially invariant beam of neutralized particles, typically argon. Material on the surface is consequently sputtered away. The rate and distribution (profile) of material removal by the ion beam is kept constant (as shown in Figure 4) and specific figures or corrections are achieved by rastering the fixed-current beam across the workpiece at varying velocities. The figuring process relies on obtaining an accurate figure error map of the workpiece surface. The solution process consists of choosing a pattern the beam traverses and determining the rastering velocities along that path. The removed material can be computed by convolving the ion beam's fixed removal profile and the rastering velocity as a function of position. The determination of the appropriate rastering velocities from the desired removal map and the known ion beam removal profile is therefore a *deconvolution* process. A unique method of performing this deconvolution was developed for the project based on research on singular expansions of filters [17]. The solution to a convolution equation can be expressed in terms of derivatives of the known function and inverse moments of the filter. The deconvolution algorithm requires information on the moments of the ion beam removal profile and a series expansion of the surface map of the work piece. A unique and stable solution is then directly available. The assumption in this algorithm is that the expansion represent the desired removal map. There is no special consideration to the geometry of the workpiece in the x-y plane. The solution provided is exact so the accuracy of expansion fit to the desired removal is the measure of the solution's accuracy.

SIMULATION RESULTS

A simulation of the process was developed to verify the algorithms and to identify important issues and parameters that are critical for the proper operation of the system. All simulations involve data from an actual 8 cm flat sample. The process of figuring the sample to ideal flat and spherical contours is then attempted by performing a discrete convolution of the ion beam removal profile and the computed solution. The resulting reduction in the RMS difference between the actual surface contour and the desired surface contour is used as the measure of the efficiency of

the process. The sample has an initial error of 234 nm RMS from a flat plane, and 113 nm RMS from a 400 m radius sphere. The expansions representing the error contours (removal map) are polynomial series. The higher the order of the series, the more accurate the solution. Initial experiments were performed to evaluate the effect of the order on the performance of the system. The number of terms used in the series expansion representing the removal map was increased and corresponding increases in the efficiency of the process were observed. The results are shown in Figure 11 as the final RMS deviation from an idealized flat plane.

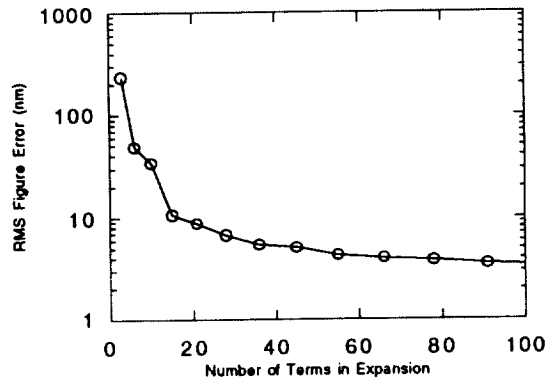


Figure 11 Results of simulation to determine effects of expansion order.

In Figure 12, the first point represents the initial RMS difference at the three expansion terms required to define a plane. The final RMS difference is directly related to the accuracy of the expansion fit. Using fifteen terms the error was reduced to 10 nm RMS and after one hundred terms to 3 nm RMS. Above approximately fifteen terms there is no significant increase in figure accuracy and 10 nm RMS is well below the accuracy of the original data. Other simulations were performed to determine the effects of systematic and random errors. The errors were introduced through the variations in the model of the beam function. The ideal beam function is modeled as a Gaussian distribution defined by two parameters: the width (λ) and the amplitude (Γ).

$$H(x,y) = \Gamma \exp\left(-\frac{x^2 + y^2}{\lambda^2}\right)$$

The sensitivity of process to systematic and random errors in the parameters is observed in Figures 12, 13 and 14. These plots depict the improvement in the RMS difference from the desired figure. This information provides a quantified measurement of the relative sensitivity to errors in the beam parameters as well as the positioning of the beam with respect to the part. Experiments are planned to verify the simulations and to provide information on the accuracy and stability of the beam parameters and positioning.

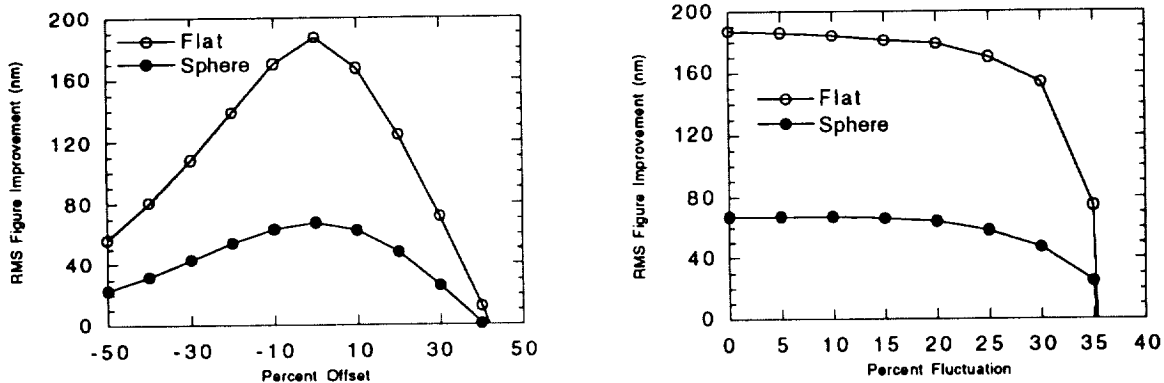


Figure 12 Simulated improvement in RMS figure error shown as a function of systematic and Normally distributed random error as a percentage of the modeled λ .

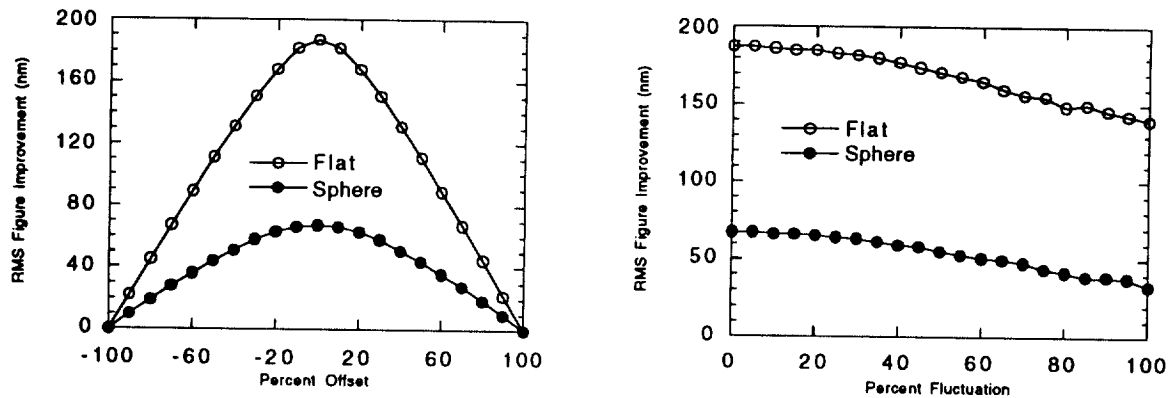


Figure 13 Simulated improvement in RMS figure error shown as a function of systematic and Normally distributed random error as a percentage of the modeled Γ .

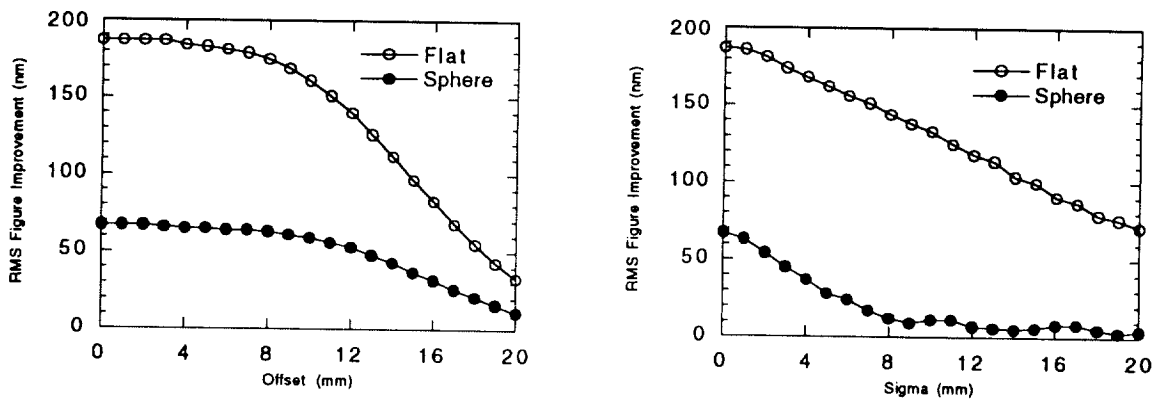


Figure 14 Simulated improvement in RMS figure error shown as a function of systematic and Normally distributed random position error.

CONCLUSIONS

It has been demonstrated that a feasible process for fabricating ceramic mirrors is to employ a deterministic ductile-grinding operation followed by a final ion beam contouring operation. A small ion machining facility has been established, and processing experiments on CVD SiC have been carried out. Removal rates for the ion beam have been characterized. The removal profile is largely gaussian in shape. CVD SiC samples were polished or micro-ground in preparation for final ion machining. Most of these pre-finished samples exhibited roughness in the 10-20 Å range. It was found that the success of the ion machining process was directly influenced by the existence of subsurface damage: samples containing subsurface damage suffered rapid deterioration in surface quality as a result of the ion machining. The observed sub-surface damage in polished samples is likely to be the residual effect of previous machining processes, rather than the direct result of polishing itself. As has been shown in previous work by many researchers, ductile grinding can produce damage-free, optical quality surfaces in SiC. Initial experiments revealed that high quality, ductile ground surfaces do not significantly roughen after removal of up to 5 μm of material by ion machining. The deconvolution algorithm for figuring optical components has been successfully developed and verified with simulations. Experiments are currently underway to validate these simulations on actual SiC and fused silica optical flats.

The proposed processing technique shows promise as a viable alternative to conventional fabrication techniques in the production of mirror components and other precision surfaces. Moreover, the results of the experiments reported here indicate that ion machining can serve as an indicator of the existence and extent of subsurface damage in

specularly finished ceramic components. Because the ion sputtering rate is dependent on material properties and atomic species, this process can be utilized for producing surface features in many different substrates. This technique is successfully utilized on a commercial basis for texturing surfaces on a relatively microscopic scale. The future of the process will be in producing macroscopic features such as optical surfaces. Another use can be found in sharpening diamond tools by the preferential etching along crystal orientation. Recent experiments performed at MSFC also used the process to produce conical ends on gradient index optical fibers by the differential etching of the varying density material. The future will only bring increasing uses for this technique. Once the groundwork has been laid, commercialization of the process will naturally follow.

ACKNOWLEDGMENTS

This work was sponsored and funded by NASA. The authors would like to express their gratitude to the following people for their support of the project; Robert Rood, Thomas Bifano, James Bilbro, Edward Montgomery, Whit Brantley, Charles Jones, Joseph Randall and Scott Wilson. Also, special thanks to Charles Griffith and Raj Khanijow who performed the tedious job of polishing the samples and to Staffan Persson who designed the support fixtures for the ion source.

REFERENCES

1. A.J. Gale, "Ion Machining of Optical Components", Optical Society of America Annual Meeting Conference Proceedings, November 1978.
2. J.R. McNeil and W.C. Herrmann, Jr., "Ion Beam Applications for Precision Infrared Optics", *Journal Vacuum Science and Technology*, 20 (3), pp. 324-326, March 1982.
3. J.R. McNeil, S.R. Wilson and A.C. Barron, "Ion Beam Figuring for Rapid Optical Fabrication", *Optical Society of America Workshop on Optical Fabrication and Testing*, pp. 62-67, October 1986.
4. S.R. Wilson, D.W. Reicher and J.R. McNeil, "Surface Figuring Using Neutral Ion Beams", *Advances in Fabrication and Metrology for Large Optics*, SPIE Vol. 966, pp. 74-81, August 1988.
5. L.N. Allen, and R.E. Keim, "An Ion Figuring System for Large Optic Fabrication", *SPIE Vol. 1168*, pp.33-50, August 1989.
6. T.J. Wilson, "New Technologies Fabricate Large Aspheres", *Laser Focus World*, Vol. 26(9), pp. 111-123, September 1990.
7. L.N. Allen, R.E. Keim T.S. Lewis and J. Ullom, "Surface Error Correction of a Keck 10m Telescope Primary Mirror Segment by Ion Figuring", *SPIE*, Vol. 1531, July 1991
8. L.N. Allen, J.J. Hannon and R.W. Wambach "Final Surface Error Correction of an Off-Axis Aspheric Petal by Ion Figuring", *SPIE*, Vol. 1543, July 1991
9. S.R. Wilson, and J.R. McNeil, "An Update on Ion Beam Figuring", *Optical Society of America Workshop on Optical Fabrication and Testing*, October 1992.
10. C.M. Egert, "Roughness Evolution of Optical Materials Induced by Ion Beam Milling", *SPIE Vol. 1752*, 1992.
11. J. Yoshioka, K. Koizumi, M. Shimizu, H. Yoshikawa, M. Miyashita, and A. Kanai, "Ultraprecision Grinding Technology for Brittle Materials: Application to Surface and Centerless Grinding Processes", *Milton C. Shaw Grinding Symposium, ASME*, Vol. 16, pp. 209-227, 1985.
12. Bifano, T.G. T.A. Dow and R.O. Scattergood, "Ductile Regime Grinding: A Technology for machining Brittle Materials", *Journal of Engineering for Industry*, Vol. 113, pp. 184-189, 1991.
13. T.G. Bifano, and S.C. Fawcett, "Specific Grinding Energy as an In Process Control Variable for Ductile Regime Grinding", *Precision Engineering*, Vol. 13(4), pp. 256-262, 1991.
14. T. G. Bifano, Kahl, W. K., and Yi, Y., "Fixed-Abrasive Grinding CVD Silicon Carbide Mirrors," submitted to *Precision Engineering*, December, 1992.
15. S.C. Fawcett, and R.W. Rood, "Ion Figuring System for Segmented, Adaptive Optics", *American Society for Precision Engineering Annual Meeting Conference Proceedings*, pp. 244-247, October 1992.
16. H.R. Kaufman, P.D. Reader and G.C. Isaacson, "Ion Sources for Ion Machining Applications", *AIAA Journal*, Vol. 15(6), pp. 843-847, June 1977.
17. R. G. Hohlfeld, J. I. F. King, T. W. Drueding, and G. v. H. Sandri, "Solution of Convolution Integral Equations by the Method of Differential Inversion", *SIAM Journal of Applied Mathematics*, 53(1), 1993.